Interplay between synchronization, observability, and dynamics

Christophe Letellier[1] and Luis A. Aguirre[2]
[1]*Université et INSA de Rouen—CORIA UMR 6614, Av. de l'Université, BP 12, F-76801 Saint-Etienne du Rouvray cedex, France*
[2]*Departamento de Engenharia Eletrônica, Universidade Federeal de Minas Gerais, Av. Antônio Carlos 6627, 31270-901 Belo Horizonte, MG, Brazil*
(Received 9 February 2010; published 7 July 2010)

Synchronizing nonidentical chaotic oscillators is very often achieved by using various types of couplings. In the practice of synchronization the "right choice" of the coupling variable—y for the Rössler system, x for the Lorenz equations, and so on—is usually stated rather than explained or justified. Using the Rössler and Rucklidge system, in this paper, it is shown that such "optimal" choices are strongly related to observability properties which, in turn, can be quantified. In this paper it will also be shown that synchronizability does not only depend on the observability of the system but it is also a consequence of the dynamical regimes under study. The paper aims at providing important insight into the critical problem of making the "right choice" when it comes to choosing the coupling variable in synchronization schemes.

DOI: 10.1103/PhysRevE.82.016204 PACS number(s): 05.45.−a

I. INTRODUCTION

Synchronization of aperiodic oscillators is a key concept that is found in many different fields (physics, biology, engineering, secure communications, etc.) and was intensively investigated since the two pioneering papers by Fujisaka and Yamada [1] and, Pecora and Carroll [2]. A review on the topic can be found in [3]. In their pioneering work, Pecora and Carroll stated, more or less explicitly, that the ability to synchronize two (identical or not) systems depended on the variable used to couple such systems [2]. In spite of the impressive amount of contributions to this topic, the required conditions to ensure a good synchronization are still lacking. When it comes to choosing the variable to be used in coupling two oscillators, there are no clear guidelines but rather one has to accept a subjective "know-how" based on which it is known that when coupling two Rössler systems

$$\begin{cases} \dot{x} = -y - z \\ \dot{y} = x + ay \\ \dot{z} = b + z(x - c) \end{cases} \tag{1}$$

the y variable should be used [2,4], but if synchronization is to be achieved between two Lorenz systems

$$\begin{cases} \dot{x} = \sigma(y - x) \\ \dot{y} = Rx - y - xz \\ \dot{z} = -bz + xy, \end{cases} \tag{2}$$

variable x should be used instead, as it provides the best results [2]. These are a couple of cases of a rather long list which makes it clear that selecting the variable to couple oscillators for synchronization is, more often than not, an *ad hoc* choice.

Recently, Sorrentino developed an adaptive coupling for achieving synchronization between two chaotic systems, and used variable x for the Rössler system and variable z for the Lorenz system without any explanation for these choices [5]. Stojanovski and colleagues were successful in using variable z for coupling two Rössler systems—which is known to provide quite bad results in general [6]. In fact, they used an observer based on the map between the original phase space $\mathbb{R}^3(x,y,z)$ and the differential embedding $\mathbb{R}^3(z,\dot{z},\ddot{z})$, that is, they in fact reconstructed the two "missing" variables x and y by using

$$\begin{cases} x = c + \dfrac{\dot{z} - b}{z} \\ y = \dfrac{\ddot{z}z^2 - \dot{z}(\dot{z} - b)}{z^2} - z \end{cases} \tag{3}$$

and, apparently, then used the three variables to obtain synchronous states between the two subsystems. Most of the systems can be treated in that way, but the Lorenz is quite difficult—if not impossible—to synchronize from y or z. This could explain why Stojanovski and co-workers only considered x as the recorded variable.

In modeling similar problems are faced, namely, that the ease with which global models from a given system are obtained strongly depends on which variable is used. Thus, it is far easier to obtain a global model from variable y of the Rössler system than from variable z. In the case of the Lorenz system, variable x is the easiest to manage and y the worse (z being excluded, because rotation symmetry is lost when using z). This led us to introduce "observability coefficients" ([7–9] among others) to help understand and quantify the quality of the system variables when it comes to reconstructing the phase space.

As an illustration, consider Takens' theorem [10] in the context of embeddings for the Rössler system. The theorem states that, a five-dimensional space which is diffeomorphically equivalent to the original three-dimensional phase space can be reconstructed from any variable. However, in practice, it is observed that it is easier to obtain a global model from variable y of the Rössler system than from variable x, and nearly impossible to achieve a global model from variable z without a strong structure selection [11]. We showed that the reason is mainly due to the nature of the map Φ between the original phase space $\mathbb{R}^3(x,y,z)$ and the m-dimensional differential embedding $\mathbb{R}^m(s,\dot{s},\ddot{s},\ldots,s^{(m-1)})$ induced by the observable s (the measured variable) [9].

A critical point in Takens' theorem is the measurement function $h:\mathbb{R}^3(x,y,z)\mapsto\mathbb{R}(s)$. The corollary proposed by Stojanovksi and his co-workers [6] presents the same critical aspect. In spite of that, the authors correctly stated that "whether two dynamical systems synchronize or not depends not only of the choice of the driving signal, but also on the underlying synchronization method." However this statement has to be linked with their comments about their corollary: "It determines *when* the synchronization is possible, but not *how*." This is a well-known problem in control theory and, for instance, the difficulty with variable z of the Rössler system can be avoided with a coordinate transformation $z\mapsto\log z=w$, because $\Phi:\mathbb{R}^3(x,y,z)\mapsto\mathbb{R}^3(w,\dot{w},\ddot{w})$ defines a global diffeomorphism. This kind of "recipes" only works in very particular cases—to the best of our knowledge, there is only another case where the log of a variable provides a "good" observable [12].

In view of this scenario, it seems fair to conclude that (i) synchronization is, at least to some extent, variable dependent; (ii) in spite of that there does not seem to be a quantitative and systematic approach to address this problem. The aim of this paper is not to propose yet another synchronization scheme, but rather to systematically investigate the different *bidirectional* couplings provided by the variables of the systems under study to check whether the conditions of synchronizability could be related—at least in part—to the observability coefficients, which are quantitative measures of aspects relevant to synchronization. Thus, it will be shown how the observability coefficients can be used to select the best variable for synchronizing two oscillators or, at least, for avoiding the worse variable. Empirical choices of coupling variables, that are not usually explained, will be now theoretically justified.

The subsequent part of this paper is organized as follows. Section II briefly introduces the concept of observability. Sections III and IV, which are the main part of this paper, are devoted to the synchronization of nonidentical systems bidirectionally coupled by a single variable. Two systems are considered, the Rössler system (Sec. III) and the Rucklidge system (Sec. IV). Section V gives a conclusion.

II. OBSERVABILITY OF DYNAMICAL SYSTEMS

A. Background

Let us start with a nonlinear system

$$\dot{x}_i = f_i(x_1,x_2,x_3), \quad i=1,2,3, \tag{4}$$

described in the three-dimensional phase space $\mathbb{R}^3(x_1,x_2,x_3)$ for the sake of simplicity and where $x_i\in\mathbb{R}$ are the dynamical variables. Assume that the observable s is obtained using the measurement function $h:\mathbb{R}^3(\boldsymbol{x})\mapsto\mathbb{R}(s)$. It is thus possible to reconstruct the phase space from the time series $\{x_i(t)\}$ using, for instance, derivative coordinates $(X=s,Y=\dot{s},Z=\ddot{s})$. The coordinate transformation between the original phase space $\mathbb{R}^3(x_1,x_2,x_3)$ and the differentiable embedding $\mathbb{R}^3(X,Y,Z)$ is defined by

$$\Phi_i \begin{cases} X = s = x_i \\ Y = \dot{s} = \dot{x}_i = f_i \\ Z = \ddot{s} = \ddot{x}_i = \dfrac{\partial f_i}{\partial x_1} f_1 + \dfrac{\partial f_i}{\partial x_2} f_2 + \dfrac{\partial f_i}{\partial x_3} f_3 \end{cases}. \tag{5}$$

Variables X, Y, and Z correspond, respectively, to the derivatives of order zero, one and two of the observable and are related to the Lie derivative of the vector field. It has been shown that the observability matrix $\mathcal{O}_i$ of a nonlinear system observed using the ith variable is exactly the Jacobian matrix of map Φ_i [9]. This correspondence is based on the observability matrix developed for nonlinear dynamical systems [13–15]. The system is thus fully observable when the determinant $\mathrm{Det}(\mathcal{J}_{\Phi_i})$ never vanishes, that is, when map Φ_i defines a global diffeomorphism (Φ_i must also be injective, a property observed in most of the cases).

When $\mathrm{Det}(\mathcal{J}_{\Phi_i})$ never vanishes, the map Φ_i can be inverted everywhere and the system can be always rewritten under the form of a polynomial jerk system

$$\begin{cases} \dot{X} = Y \\ \dot{Y} = Z \\ \dot{Z} = F_i(X,Y,Z) \\ \quad = \dfrac{\partial Z}{\partial x_1} f_1 + \dfrac{\partial Z}{\partial x_2} f_2 + \dfrac{\partial Z}{\partial x_3} f_3 \end{cases}, \tag{6}$$

where the model function $F_i(X,Y,Z)$ is free of singularities and subscript i designates the measured variable. Otherwise a jerk system might be obtained, but with singularities, that is, with a rational function F_i. This situation occurs when $\mathrm{Det}(\mathcal{J}_{\Phi_i})=0$ over some subspace in the original space: the system is said to be not fully observable.

The subspace mentioned in the previous paragraph can be of dimension 0 or higher. Two different states in such a subspace, in the original phase space, *cannot* be distinguished in the space reconstructed using the observable. It is then said that the original system cannot be fully observed from the recorded variable. From a practical point of view, even two different states that are *close* to the aforementioned subspace *are very hard to distinguish* in the reconstructed space. Therefore, in practice such a subspace corresponds to "blind spots" in the original space *when observed* through that particular variable.

Therefore the quality of an observable depends on the existence of such a singular set [of $\mathrm{Det}(\mathcal{J}_{\Phi_i})$], its dimension and its location with respect to the attractor. It is hence helpful to speak in terms of a *degree of observability* rather than in terms of a yes-or-no answer: being observable or not. As detailed in previous work (see [8,9,16] among others), it is possible to compute observability coefficients at each point of the phase space for each observable (Fig. 1). Often, the observability properties, which depend on the map Φ_i which is not too sensitive to parameter changes, usually do not depend strongly on the dynamical regime. It was therefore possible to introduce a simple procedure to compute observability coefficients directly from the Jacobian matrix of the system under study (see Appendix A).

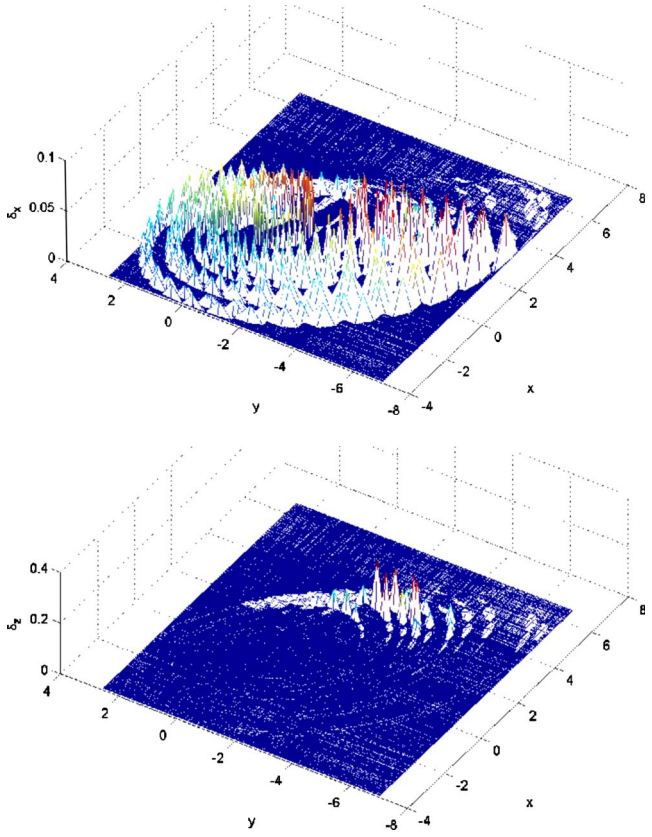

FIG. 1. (Color online) Observability coefficients δ_x and δ_z projected onto the $x-y$ plane. Higher peaks indicate higher observability. δ_x (δ_z) measures the local observability when only variable x (z) is used. Case of the Rössler system with $a=0.52$, $b=2$, and $c=4$.

B. Example

Let us describe a simple example to explain how observability can affect the quality of the synchronization in the case of the Rössler system. When the observable is variable y the case is very simple since map $\Phi_y:\mathbb{R}^3(x,y,z)\mapsto\mathbb{R}^3(y,\dot{y},\ddot{y})$ defines a global diffeomorphism [$\mathrm{Det}(\Phi_y)\neq 0,\ \forall x\in\mathbb{R}^3$]. The Rössler system is, therefore, fully observable from variable y. In that case, the observability coefficient is constant over the whole phase space. This is not the case for variable x and z. The observability coefficients were computed over a trajectory for these two latter variables (Fig. 1). From variable x the Rössler dynamics is only observable when the trajectory evolves along the unstable manifold of the inner fixed point (mainly parallel to the $x-y$ plane). When the trajectory leaves that plane, the observability coefficient δ_x becomes nearly null, indicating that, in practice, x conveys very little information about how the other variables of the system evolve off the unstable manifold of the inner fixed point [Fig. 1(a)].

The case where the Rössler attractor is observed through variable z is the complement to the previous situation. This variable—that is, by definition orthogonal to the $x-y$ plane, has no information on the evolution of the others while the trajectory is along the unstable manifold of the inner fixed point. This is confirmed by the observability coefficient that nearly vanishes in this region of phase space [Fig. 1(b)]. Consequently, variable z only conveys sufficient information during the bursts along the z axis.

Now consider the case in which bidirectional synchronization is performed using a given variable s. If the observability coefficient δ_s is low there might not be sufficient information transmitted from the first oscillator to the second, and vice versa. In other words, the dynamics of one oscillator will be very hard to "recognize" by the other oscillator whenever the state of the first system is close to "blind spots" of the first system. When a poor observable is used to couple two systems, it could become very difficult to achieve synchronization because the two systems are only sporadically coupled. As pointed out by Parlitz and co-workers [17], a sporadic driving considerably reduces the amount of information transmitted from one system to the other and thereby our ability to obtain a good synchronization. These features explain why many works devoted to synchronization of two nonidentical Rössler systems use y coupling (see [2,4] for instance). From the observability point of view, good synchronization would not be expected when a coupling through variable z is used.

III. SYNCHRONIZATION OF TWO NONIDENTICAL RÖSSLER SYSTEMS

Let us start with two coupled nonidentical Rössler systems

$$\dot{x}_{1,2}=\omega_{1,2}[-y_{1,2}-z_{1,2}]+\rho_x(x_{2,1}-x_{1,2})$$

$$\dot{y}_{1,2}=\omega_{1,2}[x_{1,2}+ay_{1,2}]+\rho_y(y_{2,1}-y_{1,2})$$

$$\dot{z}_{1,2}=\omega_{1,2}[b+z_{1,2}(x_{1,2}-c)]+\rho_z(z_{2,1}-z_{1,2}), \qquad (7)$$

where the subindices indicate the system, e.g., $x_{1,2}$ stands for both x_1 and x_2. Parameters ω_1, ω_2, and ρ_s are constant. Bidirectional couplings are, thus, here considered. In system Eq. (7), $\omega_{1,2}$ will be used to slightly detune the two oscillators. As in [4], we use $\delta\omega=\omega_2-\omega_1=0.04$ with $\omega_1=1$. In this paper, the bidirectional coupling was applied to a single variable, that is, a single ρ_s was nonzero. Only nonzero terms will be reported.

A. Complete synchronization

Complete synchronization is the simplest and the strongest form among the different kinds of synchronization. It corresponds to a regime where the two oscillators present synchronous states [18]: the synchronous state $\boldsymbol{x}_1=\boldsymbol{x}_2$ is established only when the coupling parameter ρ exceeds a critical value. Pecora and Carroll explicitly wrote that "only the y drive configuration will synchronize" [2]. As we will see, this was also observed with our bidirectional coupling term in the case of a funnel Rössler attractor (Fig. 2).

We started our study by checking whether the synchronizability between two non-identical Rössler systems depends on the dynamical regime. The latter was varied by increasing the value of the bifurcation parameter a from $a=0.36$ (first limit cycle of the period-doubling cascade) to $a=0.555$, just before the ejection to infinity that occurs at $a=0.556$. For the

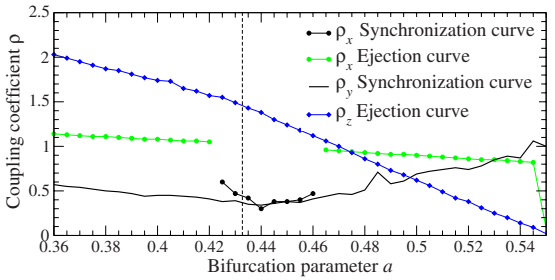

FIG. 2. (Color online) Critical coupling curves that correspond to the onset of synchronization (synchronization curve) and the ejection of the trajectory to infinity (ejection curve), respectively. Below the synchronization curve, the average distance between points and the first bisecting line of plane y_1-y_2 is greater than 0.1. Case of the Rössler system, $b=2$, $c=4$, and $\delta\omega=0.04$.

largest values, the attractor boundary was very close to the boundary of the attraction basin and it is nearly impossible to perturb the dynamics—to attempt synchronization—without provoking an ejection to infinity as shown by the ejection curve when the two systems are coupled with variable x. For this reason, in the case of the x variable, two critical curves have to be plotted: (i) if complete synchronization occurs, we show the ("synchronization curve") lowest value of the coupling terms ρ_0 for which this happens. To decide if complete synchronization had occurred we compute the mean distance δ between the state and the first bisecting line on the plane y_1-y_2. If $\delta<0.1$, the two nonidentical oscillators were considered as completely synchronous. On the other hand, ii) if complete synchronization did *not* happen, we show the ("ejection curve") coupling strength ρ_∞ at which the trajectory was ejected to infinity. This means that, for the particular value of the bifurcation parameter, if $\rho_x<\rho_\infty$ the coupled system is stable but is *not* synchronized, and if $\rho_x\geq\rho_\infty$ the coupled system becomes unstable.

When the two oscillators were y-coupled, complete synchronization was obtained (Fig. 2) for all dynamical regimes between the first period-doubling cascade and the ejection of the trajectory to infinity (=0.556). The critical coupling parameter $\rho_{y,0}$ has its minimal value when the symbolic dynamics built on the unimodal map is complete, that is, for $a=0.43295$ [19]. Beyond this a value, the dynamics becomes multimodal and is phase noncoherent. It was observed that the critical coupling $\rho_{y,0}$ increased as the dynamics was developed. This is not so surprising since it is known that phase noncoherent attractors are more difficult to synchronize than coherent attractors [4]. This feature confirms that synchronizability depends on the dynamics.

When variable x was used to couple the two nonidentical Rössler systems, complete synchronization was only obtained over the range $a\in[0.425;0.455]$ (Fig. 3) that corresponds to a situation for which the neighborhood of the inner fixed point is visited during quite a long time. As previously seen, this neighborhood of the inner fixed point corresponds to the domain where the dynamics is observable. Bursts associated with excursions of the trajectory outside the unstable manifold of the inner fixed point where the observability is poor are thus too sparse and short to prevent synchronization of the two subsystems. Outside this range, it was not

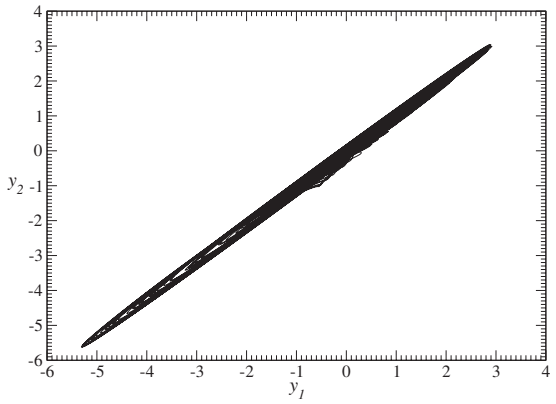

FIG. 3. Projection on the y_1-y_2 plane of the attractor solution to the coupled non-identical Rössler systems when ρ_x is at its minimal value for a successful complete synchronization (Fig. 2). Both systems are, thus, synchronous to produce a chaotic attractor very close to the attractor solution to the original Rössler system. Parameter values: $a=0.455$, $b=2$, $c=4$, $\rho_{x,0}=0.51$, and $\delta\omega=0.04$.

possible to achieve complete synchronization. At a rather constant coupling strength ($\rho\approx1$), the trajectory was ejected to infinity before achieving complete synchronization.

When the two oscillators were coupled via variable z, it was never possible to obtain a complete synchronization. The critical coupling ρ_∞ at which the trajectory was ejected monotonically decreases with a. In a certain sense, it reflects the distance between the attractor boundary and the boundary of the attraction basin. A typical behavior observed just before the crisis is shown for $a=0.36$. For this parameter value the *uncoupled* oscillators settle to a limit cycle which is quite far from the boundary of the attraction basin. However, when coupled, depending on the coupling strength the solution of the coupled pair is ejected to infinity. Let us call ρ_∞ the critical coupling in such a way that values greater than ρ_∞ will eject the system to infinity. If we choose to couple the system with a value slightly smaller than the critical value, that is, $\rho_z\leq\rho_\infty$ the result is a non synchronous (hyperchaotic) state (Fig. 4). Therefore, in this case, even just before ejection the oscillator are far from being synchronized.

The monotonic decrease of the ejection threshold for ρ_z results from the fact that the boundary crisis occurs in the neighborhood of the outer fixed point, a point that is approached when the trajectory leaves the $x-y$ plane. The ejection limit is in fact proportional to the distance between the attractor boundary and the stable manifold of the outer fixed point. At $a=0.55$, the attractor is very close to this manifold, and the smallest perturbation is sufficient to send the trajectory across the manifold.

Complete synchronization was easily obtained when the two systems were coupled using variable y; was only obtained over a rather small range of parameter a when variable x was used, and it was never achieved using z. Therefore, to achieve complete synchronization, the best variable for coupling the two Rössler systems is y, the worse is z, and variable x is somewhere in between. This is exactly the order provided by the observability coefficients: $\eta_{y^2}=1$, $\eta_{x^2}=0.88$ and $\eta_{z^2}=0.44$. Complete synchronization thus also depends on how the oscillator dynamics are "seen" through the vari-

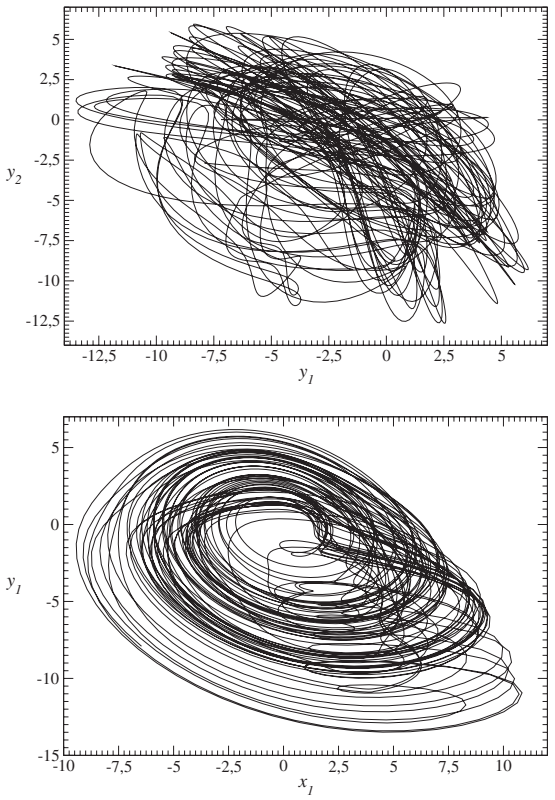

FIG. 4. Solution to the six-dimensional system when the coupling term is at its largest value before the ejection of the trajectory to infinity. Parameter values: $a=0.36$, $b=2$, $c=4$, $\rho_z=1.05\leq\rho_\infty$, and $\delta\omega=0.04$.

ables used to couple the oscillators. This is quantified by observability coefficients.

B. Cross-section synchronization

Although complete or identical synchronization is simple to understand and to define, unfortunately such a behavior is often too demanding, especially for simple coupling schemes such as the one used in Eq. (7). For the purposes of this paper it is important not to increase the complexity of the coupling used to synchronize the two systems. Therefore, alternative definitions of synchronization should be sought. A commonly used definition is that of phase synchronization [18]. Unfortunately, when the dynamics is nonphase coherent, it is rather tricky to define a phase [4,20], mainly because the trajectory spirals around the inner fixed point and a curve connecting the latter to the outer fixed point [21]. For this reason, alternative definitions of phase were required, as the one proposed by Osipov and his co-workers based on the curvature of the trajectory [4].

In what follows, an alternative approach will be sought in order to be able to define phase synchronization even in the case of phase-non-coherent dynamics. The aforementioned approach is based on the fact that a proper Poincaré section for Rössler attractors can be defined in a way that is independent on the dynamics [19]. This directly results from the fact that, although the dynamics is phase noncoherent, funnel Rössler attractors can be enclosed by a genus-1 bounding

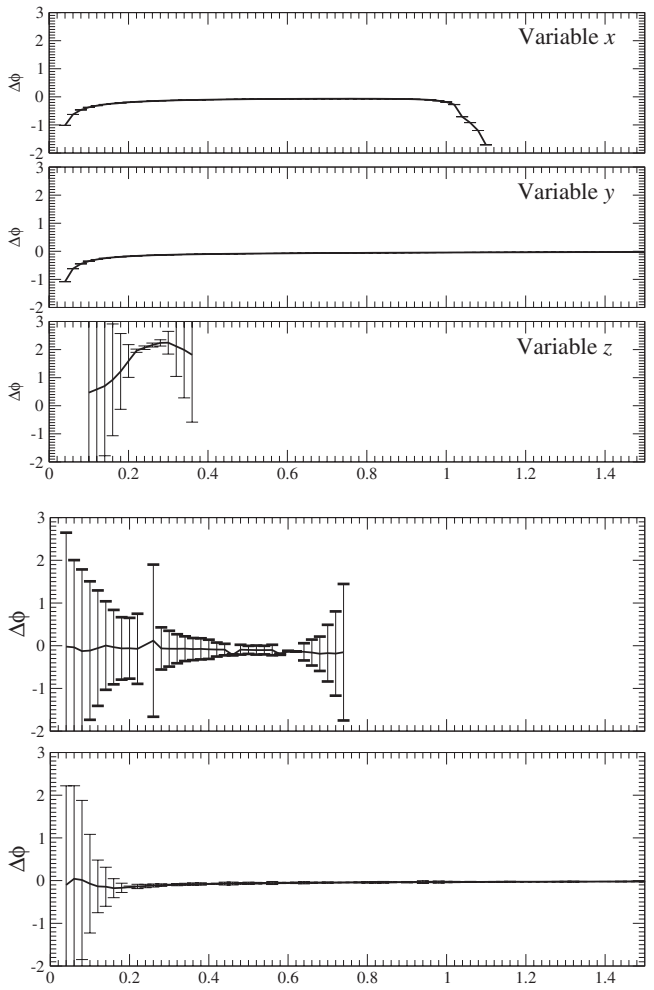

FIG. 5. Mean phase shift $\Delta\phi$ versus the coupling strength computed for the three variables of the spiral and funnel Rössler attractors. The bars indicate $\pm\sigma$ where σ is the standard deviation. Other parameter values: $b=2$ and $c=4$. In (b) the top plot refers to coupling with x and the bottom one is for y couplings.

torus leading to a single component Poincaré section (see Appendix B). From this point of view, it seems natural to consider a Poincaré section related phase [19,22].

According to a procedure described in [18], it is possible to define a phase based on a Poincaré section as follows. The time interval between two intersections of the trajectory with the Poincaré section corresponds to one complete oscillation; therefore the phase increase during this time interval is exactly 2π rad. Hence, we can assign to the time T_k the values of the phase $\phi(T_k)=2\pi k$ rad. For an arbitrary instant of time $T_k<t<T_{k+1}$, the phase is just provided by a linear interpolation between these values [23],

$$\phi(t)=2\pi k+2\pi\frac{t-T_k}{T_{k+1}-T_k}(\text{rad}). \tag{8}$$

It is believed that the relevant dynamical features—especially recurrence properties —are more efficiently investigated on a Poincaré section [24]. This motivated our choice for using linearized phase ϕ. We will thus refer to "cross-section-synchronized" systems when the linearized phase er-

ror between such systems, $\phi_2 - \phi_1$, remains around zero and is nearly constant.

As before, we varied the coupling (nature and strength) and verified if cross-section synchronization was attained. In the case of phase coherent attractors [Fig. 5(a)] we observed that it is very easy to obtain cross-section synchronization using y a the coupling variable. The robustness of the synchronization was slightly less with two x-coupled subsystems. But it was nearly impossible to obtain cross-section synchronization using the z variable. A very narrow range of coupling strength around $\rho_z = 0.26$ led to a nearly constant but not null phase shift.

A different situation was observed for phase noncoherent attractors [Fig. 5(b)]. Cross-section synchronization was possible using the y variable for values of coupling strength in the range $\rho_y \in]0.2;1.5[$. Using x to couple the oscillators resulted in cross-section synchronization for $\rho_x \approx 0.6$ and no such synchronization was obtained using z couplings. Once again, the synchronizability—here of the cross-section type—depends on the dynamical regime and on the observability of the dynamics through the coupling variable.

IV. TWO NONIDENTICAL RUCKLIDGE SYSTEMS

The Rucklidge system is reviewed in Appendix C. This is a Lorenz-like system with a rotation symmetry $\mathcal{R}_z(\pi)$. As a consequence, variable z is left invariant under the symmetry and it is not possible to know on which spiral the trajectory is. This specific dynamical property is not taken into account by observability coefficients [16]. Another interesting topological property that the Rucklidge system has—like most of Lorenz-like systems [26]—is that, depending on its parameter values, it can produce a genus-1 or a genus-3 attractor (see Appendix C). In the former case, the trajectory always visits one spiral after the other, for one revolution each. In the latter, transitions from one spiral to the other occur chaotically. As we may expect, such dynamical characteristics will have a strong impact on the synchronizability of two nonidentical Rucklidge systems.

A. Complete synchronization

The observability coefficients computed for the Rucklidge system (see Appendix A) are:

TABLE I. Coupling strengths corresponding to the best synchronization obtained with the different couplings. Case of two nonidentical Rucklidge systems.

Observability coefficients	Genus-one	Genus-three
$\eta_{x^2}=0.88$	$\rho_{x,0}=1.4$ Complete	$\rho_{x,0}=0.6$ Complete
$\eta_{z^2}=0.44$	$\rho_{z,0}\approx 10.5$ Nearly complete	Never complete
$\eta_{y^2}=0.34$	$\rho_{y,0}=18.0$ Complete	$\rho_{y,0}=5.0$ Complete

$$\eta_{x^2} = 0.88 > \eta_{z^2} = 0.44 > \eta_{y^2} = 0.34. \quad (9)$$

According to them, complete synchronization should be easier with an x-coupling (Table I) than using the other variables. This remained true for genus-one and genus-three attractors.

Synchronization of two non-identical Rucklidge systems with z-couplings was nearly achieved for the genus-one attractor [Fig. 6(a)] but never in the case of the genus-three attractor [Fig. 6(b)]. The fact that significantly better results were obtained with the genus-one attractor was not so surprising: in this case, the trajectory does not visit the neighborhood of the saddle fixed point at the origin of the phase space and, consequently, does not leave any possibility to the two subsystems to drastically diverge one from the other even with a lack of information on the location of the trajectory. In spite of the symmetry, the case is nearly similar to the case of systems without symmetry.

When the genus-three attractor was considered, it was not possible to obtain a complete synchronization with z-coupled subsystems. The information transmitted by variable z contains nothing about which spiral is visited, the two subsystems are therefore "π phase free." In a chaotic manner, a π phase shift is induced when the trajectory visits the neighborhood of the saddle fixed point, preventing any complete synchronization.

Thus, when the two subsystems are not π phase-shift—case of the genus-one attractor—the synchronizability is in agreement with observability coefficients. Such a result does not remain true for the genus-three attractors since there is a strong dynamical property—the lack of information in variable z about the spiral actually visited—that prevents any

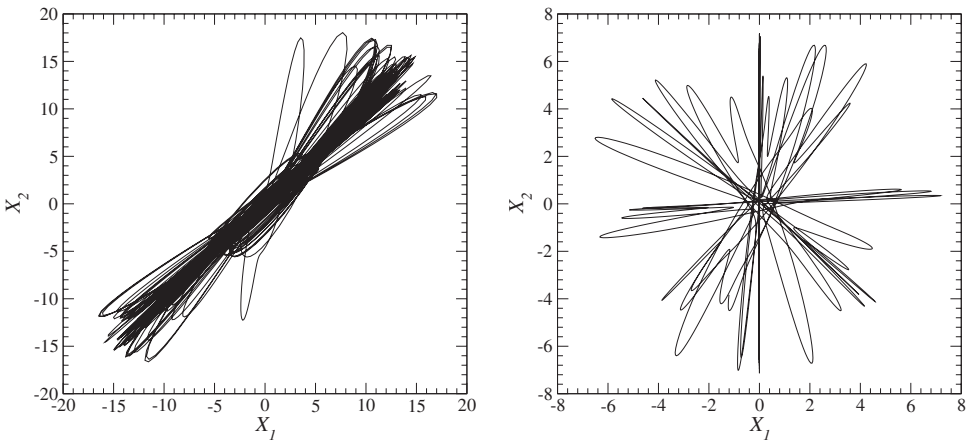

FIG. 6. Best cross-section synchronization obtained with two z-coupled nonidentical Rucklidge systems. Parameter values: (a) $\lambda = -6.7$ and $\kappa = -2$ and, (b) $\lambda = -39.7$ and $\kappa = -4.4$.

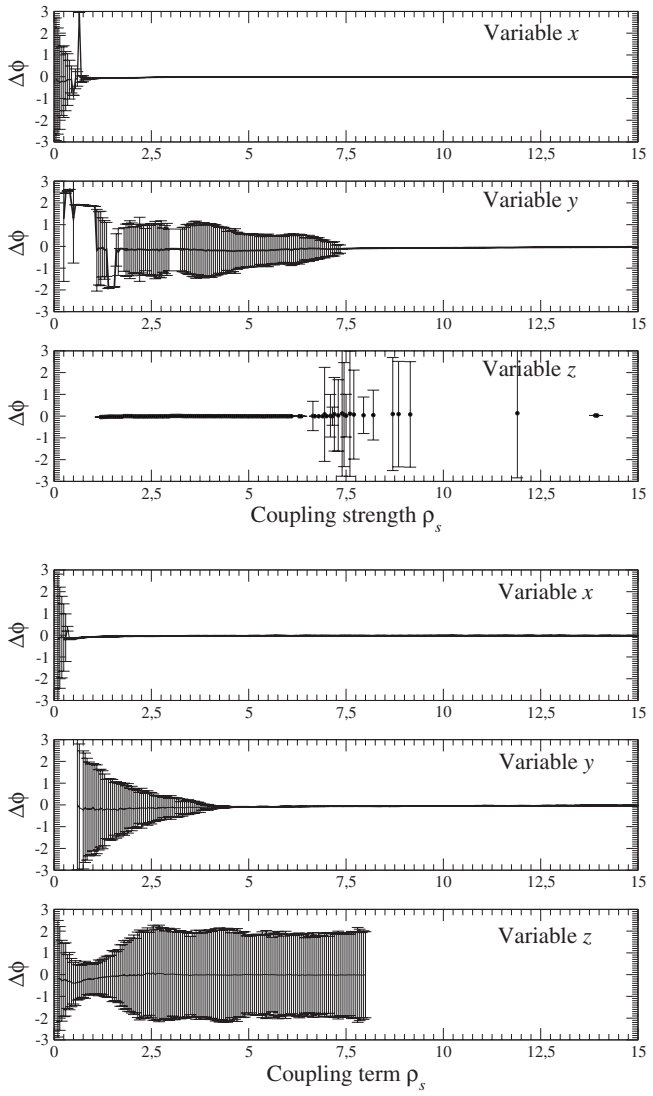

FIG. 7. Mean phase shift computed for the three different type of couplings and the two type of attractors produced by the Rucklidge system.

complete synchronization in spite of a rather good observability. Such a feature is associated with the lack of (global) observability which, unfortunately, is not measured by our coefficients [16].

B. Cross-section synchronization

Depending on the genus of the bounding torus enclosing the attractor, the global Poincaré section has one or two components. The phase ϕ is set to 0 in each of the components. The analysis is then performed in a similar way as for the Rössler system. The mean phase shifts $\Delta\phi$ with their standard deviation are reported in Figs. 7(a) and 7(b) for the genus-one and genus-three attractors, respectively. The critical coupling strengths at which the cross-section synchronization was obtained are reported in Table II, where the observability coefficients are reprinted.

As observed with complete synchronization, in the case of genus-one attractor, the critical strength to cross-section synchronize the two subsystems is in agreement with the quality of the coupling variable and cross-section synchronous states can be obtained with the three variables. It is interesting to notice that such critical strength is related to the cost of synchronization [27] which not only depends on the similarity of the dynamics being synchronized but also, as shown in this paper, it depends on the coupling variable. The situation is slightly less obvious with the genus-three attractor since, as expected, it was not possible to perfectly cross-section synchronize the two subsystems [the standard deviation always remained significantly large as shown in Fig. 7(b)] using variable z. This last example thus confirmed that the synchronizability of two nonidentical systems depends on both the observability induced by the coupling variable and on the dynamics.

TABLE II. Critical coupling coefficients $\rho_{s,0}$ at which the two nonidentical Ruklidge systems were cross-section synchronized (or nearly in one case).

Observability coefficients	Genus-one	Genus-three
$\eta_{x^2}=0.88$	$\rho_{x,0}\approx 0.75$	$\rho_{x,0}=0.1$
$\eta_{z^2}=0.44$	$\rho_{z,0}\approx 1.25$	$\rho_{z,0}=1.0$ Not perfect
$\eta_{y^2}=0.34$	$\rho_{y,0}=7.5$	$\rho_{y,0}=4.5$

V. CONCLUSION

Since the seminal paper by Pecora and Carroll it is known that synchronizability depends somehow on the coupling variable. But the reasons for that seem not to be known. Using observability coefficients that quantify the quality of a phase space induced by a given variable, we showed that a significant part of this dependence can be explained. However, such coefficients cannot explain everything. In fact, it is also known that synchronizability depends on dynamical properties, as phase coherence, to which observability measures are essentially insensitive.

These ideas were illustrated with two worked examples. In such examples it was shown that two dynamical properties that can affect the synchronizability are the phase coherence and the symmetries. The clear dependence between observability and the ability to synchronize two systems is believed to be quite general. In fact, the strong correlation between observability coefficients and the ability of modeling from one recorded variable using a sufficiently general model class has been verified for a large number of different systems. The dependence between observability and synchronizability might be blurred by the underlying dynamics which also play an important role.

General conclusions can be proposed as follows. When the attractor is phase-coherent (bounded by a genus-one torus and characterized by a unimodal map), the synchronizability is in agreement with the observability coefficients; in particular, an observability coefficient close to one ensures us to be able to synchronize two nonidentical systems. In the other extreme cases, as the observability coefficient becomes smaller, it is good synchronization becomes gradually harder

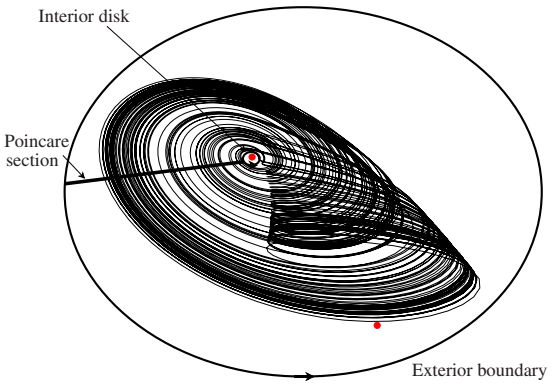

FIG. 8. (Color online) Genus-one bounding torus enclosing the funnel Rössler attractor. Parameter values: $a=0.520$, $b=2$, and $c=4$

and could become nearly impossible for very low observability.

It is not yet completely possible to address the problem analytically, and since synchronizability is dynamics dependent, a general theory might not be "just around the corner." On the other hand, by using concepts related to observability of nonlinear dynamics and the quantification provided by observability coefficients, it is believed that a significant step forward was given in the direction of improving our insight to the problem of synchronizability and suggesting tools to further investigate it.

ACKNOWLEDGMENTS

C. Letellier and L. A. Aguirre are partly supported by CNRS and CNPq. C.L. thanks Syamal Dana for stimulating discussions.

APPENDIX A: ESTIMATION OF THE SYMBOLIC OBSERVABILITY COEFFICIENTS

In this appendix, we propose an algorithmic procedure to compute the symbolic observability coefficients. This procedure is obtained from the procedure detailed in [28]. It is here explained for three-dimensional (3D) systems.

Step 1, write the so-called fluency matrix by replacing each (non)constant element of the Jacobian matrix with $(\bar{1})1$, and zero otherwise. This corresponds to (non)linear terms in the vector field.

Step 2, choose a variable to "reconstruct" the dynamics. Define a column vector C_1 where 1 corresponds to the "measured" variable and 0 otherwise. Then replace the diagonal element of the fluence matrix F corresponding to this variable by a dot and multiply each row of it by the corresponding element in C_1. The matrix H_1 is thus obtained.

Step 3, count the number p_1 of linear elements and the number q_1 of nonlinear elements in H_1.

Step 4, replace the dot in H_1 by 0, 1 or $\bar{1}$ according to the Jacobian matrix, and transpose H_1.

Step 5, count the sum of the elements of each row, both 1 and $\bar{1}$ should be counted as 1. This defines the new column vector C_2.

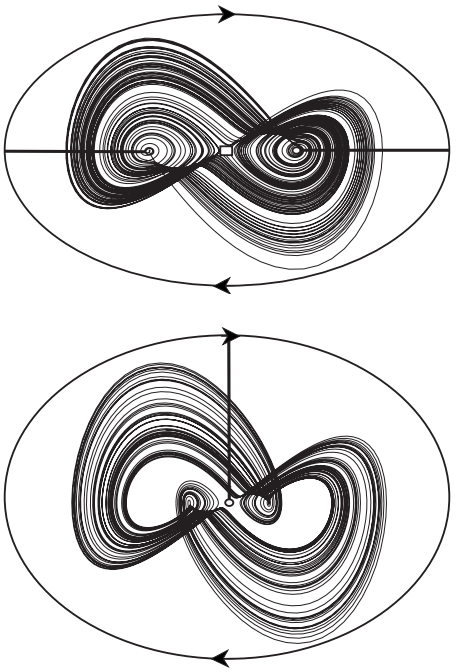

FIG. 9. Two topologically inequivalent attractors solution to the Rucklidge system. Parameter values: (a) $\lambda=-6.7$ and $\kappa=-2$ and, (b) $\lambda=-39.7$ and $\kappa=-4.4$.

Step 6, H_2 is obtained by (i) replacing each nonzero element of H_1^T by a dot and (ii) replacing each remaining element by its corresponding element in the fluence matrix multiplied by the corresponding element of the column vector C_2.

Step 7, count the number p_2 of 1 and the number q_2 of $\bar{1}$.

Step 8, the observability coefficient is thus given by

$$\eta=\frac{1}{2}\left[\frac{p_1}{p_1+q_1}+\frac{q_1}{(p_1+q_1)^3}+\frac{p_2}{p_2+q_2}+\frac{q_2}{(p_2+q_2)^2}\right],$$

where p_i+q_i is replaced with q_i+1 when $p_i=0$.

Example: The Rucklidge system Eq. (C1) has a Jacobian matrix equal to

$$J=\begin{bmatrix}0 & 1 & 0\\ -\lambda+z & \kappa & -x\\ -2x & 0 & -1\end{bmatrix}.$$

Step 1, the fluence matrix F is

$$F_{ij}=\begin{bmatrix}0 & 1 & 0\\ \bar{1} & 1 & \bar{1}\\ \bar{1} & 0 & 1\end{bmatrix}.$$

Step 2, let us choose variable y. Thus, we have $C_1=\begin{bmatrix}0\\1\\0\end{bmatrix}$, and

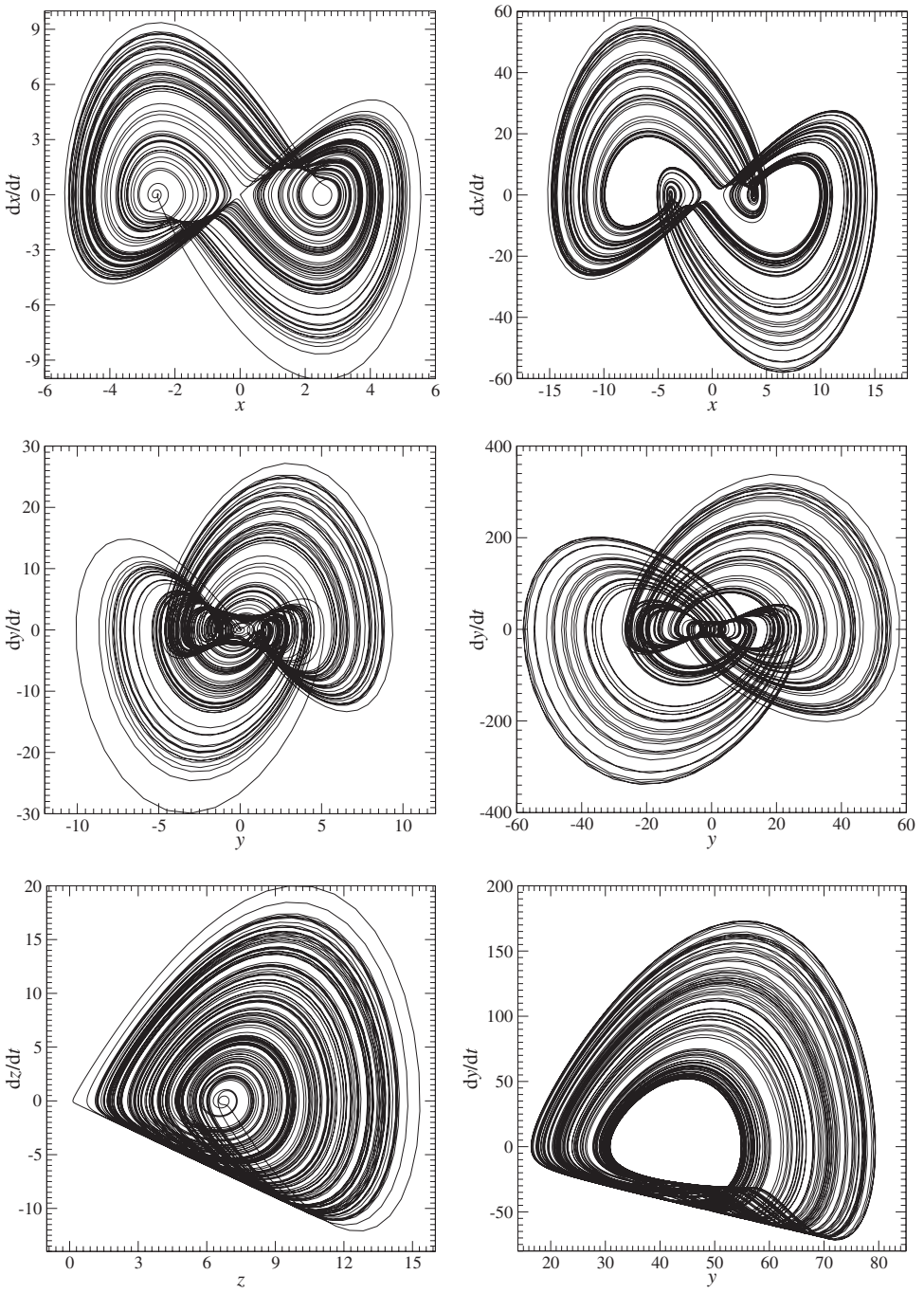

FIG. 10. Chaotic attractors solution to the Rucklidge system. Parameter values: (a) $\lambda=-6.7$ and $\kappa=-2$ and, (b) $\lambda=-39.7$ and $\kappa=-4.4$.

$$H_1=\begin{bmatrix}0 & 0 & 0\\ \bar{1} & \cdot & \bar{1}\\ 0 & 0 & 0\end{bmatrix}.$$

Step 3, $p_1=0$ and $q_1=2$.

Step 4, we replace the dot in H_1 with 1, and we then transpose the matrix to obtain

$$H_1^T=\begin{bmatrix}0 & \bar{1} & 0\\ 0 & 1 & 0\\ 0 & \bar{1} & 0\end{bmatrix}.$$

Step 5 $C_2=\begin{bmatrix}1\\ 1\end{bmatrix}$.

Step 6

$$H_2=\begin{bmatrix}0 & \cdot & 0\\ \bar{1} & \cdot & \bar{1}\\ \bar{1} & \cdot & 1\end{bmatrix}.$$

Step 7 $p_2=1$ and $q_2=3$.

Step 8

$$\eta_{y^2} = \frac{1}{2}\left[\frac{0}{2} + \frac{2}{2^3} + \frac{1}{4} + \frac{3}{4^2}\right] = 0.34.$$

APPENDIX B: SPIRAL AND FUNNEL RÖSSLER ATTRACTORS

The Rössler equations [25]:

$$\begin{cases} \dot{x} = -y - z \\ \dot{y} = x + ax \\ \dot{z} = b + z(x - c) \end{cases}, \tag{B1}$$

produces different chaotic attractors depending on the parameter values [19,22]. This system has two fixed points

$$F_{\pm} = \begin{vmatrix} x_{\pm} = az_{\pm} \\ y_{\pm} = -z_{\pm} \\ z_{\pm} = \dfrac{c \pm \sqrt{c^2 - 4ab}}{2a} \end{vmatrix}. \tag{B2}$$

F_- is the inner fixed point—that is surrounded by the attractor—and F_+ is the outer fixed point. The stable manifold of the latter corresponds to a part of the attraction basin boundary. A curve—corresponding to the vortex around which secondary oscillations take place—can be identified [21]. As investigated by Farmer and his co-workers [29], one can distinguish phase coherent regime ($0.126 < a < 0.43295$) and phase noncoherent regimes ($0.43295 < a < 0.556$) for $b=2$ and $c=4$ [19]. Phase coherent attractors correspond to a simple topology—the simplest suspension of a logistic map—and are characterized by a well-pronounced peak in the power spectrum. Phase noncoherent attractors are associated with more complicated topologies—for instance, they correspond to the simplest suspension of a three-modal map for $a=0.520$ [19]—and have rather broad band spectra. Rössler designated coherent attractors by "spiral attractor" and phase noncoherent attractors by "funnel" attractors [30].

Chaotic attractors can be described in terms of branched manifolds (or template) which, in turn, are enclosed in bounding tori. The latter serve to organize branched manifolds in the same way that branched manifolds organize periodic orbits embedded within chaotic attractors [31]. All Rössler attractors—coherent as well as noncoherent— re enclosed in a genus-one bounding torus as shown in Fig. 8. This represents a projection of a two-dimensional surface without self-links in $\mathbb{R}^3$ down onto a plane. The projection can always be brought in a canonical form [31,32]. Such projection is made of the outer boundary of a disk and g interior disks. These interior disks are of two types: n_c circles around which the flow is in the same direction as the flow on the exterior boundary, and n_p interior polygons with $2n$ sides ($n>1$) and $2n$ singularities. The former correspond to a point of a focus type and the latter to a point of saddle type. An illustrative example (Fig. 9) will be provided in Appendix C devoted to the Rucklidge system. The relevant point is that the "global" Poincaré section of any flow bounded by a genus-g torus has $g-1$ disconnected components [31,32] (for $g \geq 3$ and one for $g=1$; there is no genus-2 bounding torus). Component of the global Poincaré section always connect one circle interior disk to the exterior boundary.

APPENDIX C: THE RUCKLIDGE SYSTEM

In his investigation to model different configurations of convection, Rucklidge proposed the set of differential equations [33].

$$\begin{cases} \dot{x} = y \\ \dot{y} = -\lambda x + \kappa y - xz \\ \dot{z} = -z + x^2 \end{cases}, \tag{C1}$$

that has an algebraic structure quite close to the structure of the Lorenz system. This Lorenz-like system is invariant under a rotation symmetry around the z axis as the Lorenz system is. This system has three fixed points, one located at the origin of the phase space and two symmetry related with coordinates $x_{\pm} = \pm\sqrt{-\lambda}$, $y_{\pm}=0$ and $z_{\pm}=-\lambda$.

Like the Lorenz system, depending on its parameter values, the Rucklidge system may produce two topologically inequivalent attractors. The first one is a "Lorenz-like attractor" [Fig. 9(a)]. It can be enclosed by a genus-three bounding torus and, consequently, its global Poincaré section has two components that may be chosen as shown in Fig. 9(a). This attractor is a double suspension of a Lorenz map. The second attractor [Fig. 9(b)] is topologically equivalent to the so-called "Burke and Shaw attractor" [34]. This attractor is enclosed by a genus-one bounding torus. Like Rössler attractors, the global Poincaré section has a single component as shown in Fig. 9(b). This attractor is a double suspension of a unimodal map with a differentiable maximum.

The x-induced embedding [Fig. 10(a)] provides a clear representation of the attractor structure and its symmetry. It can be easily seen that the Lorenz-like attractor can be bounded by a genus-3 torus. Each of the three holes are associated with one fixed point (see [31] for more details). The "Burke and Shaw" attractor is bounded by a genus-1 torus. It is therefore easier to define a phase in the latter case. This will have consequences when attempt to synchronize two Rucklidge systems.

The y-induced embedding [Fig. 10(b)] still presents a clear representation of the symmetry of the attractors but the central structure of the attractor is blurred. This results directly from the fact that the three fixed points are not distinguished by variable y. The z induced embedding [Fig. 10(c)] provides a clear representation of the attractor structure but the symmetry is modded out. This means that there is no information in variable z about in which spiral the trajectory is located. From the observability point of view, this means that two different states in $\mathbb{R}^3(x,y,z)$ cannot be distinguished in $\mathbb{R}^3(z,\dot{z},\ddot{z})$.

[1] H. Fujisaka and T. Yamada, Prog. Theor. Phys. **69**, 32 (1983).
[2] L. M. Pecora and T. L. Carroll, Phys. Rev. Lett. **64**, 821 (1990).
[3] S. Boccaletti, J. Kurths, G. Osipov, D. L. Valladares, and C. S. Zhou, Phys. Rep. **366**, 1 (2002).
[4] G. V. Osipov, B. Hu, C. Zhou, M. V. Ivanchenko, and J. Kurths, Phys. Rev. Lett. **91**, 024101 (2003).
[5] F. Sorrentino, Phys. Rev. E **80**, 056206 (2009).
[6] T. Stojanovski, U. Parlitz, L. Kocarev, and R. Harris, Phys. Lett. A **233**, 355 (1997).
[7] L. A. Aguirre, IEEE Trans. Educ. **38**, 33 (1995).
[8] C. Letellier, J. Maquet, L. Le Sceller, G. Gouesbet, and L. A. Aguirre, J. Phys. A **31**, 7913 (1998).
[9] C. Letellier, L. A. Aguirre, and J. Maquet, Phys. Rev. E **71**, 066213 (2005).
[10] F. Takens, Lect. Notes Math. **898**, 366 (1981).
[11] C. Lainscsek, C. Letellier, and I. Gorodnitsky, Phys. Lett. A **314**, 409 (2003).
[12] M. Lefranc, D. Hennequin, and P. Glorieux, Phys. Lett. A **163**, 269 (1992).
[13] C. Lobry, SIAM J. Control **8**, 573 (1970).
[14] H. J. Sussmann and V. J. Jundjeric, J. Differ. Equations **12**, 95 (1972).
[15] A. J. Krener, SIAM J. Control **12**, 43 (1974).
[16] C. Letellier and L. Aguirre, Chaos **12**, 549 (2002).
[17] U. Parlitz, L. Kocarev, T. Stojanovski, and L. Junge, Physica D **109**, 139 (1997).
[18] A. Pikovsky, M. Rosenblum, and J. Kurths, *Synchronization—A Universal Concept in Nonlinear Sciences* (Cambridge University Press, Cambridge, England, 2003), pp. 144–154.
[19] C. Letellier, P. Dutertre, and B. Maheu, Chaos **5**, 271 (1995).
[20] M. C. Romano, M. Thiel, J. Kurths, I. Z. Kiss, and J. L. Hudson, EPL **71**, 466 (2005).
[21] R. Gilmore, J.-M. Ginoux, T. Jones, C. Letellier, and U. S. Freitas, J. Phys. A: Math. Theor. **43**, 255101 (2010).
[22] R. Barrio, F. Blesa, and S. Serrano, Physica D **238**, 1087 (2009).
[23] This procedure was introduced as being particularly well suited to the case of ECG for which few waves (P, Q, R, S, and T according to Einthoven's labeling) can be identified. This is exactly what we have when the Rössler attractor is multimodal. There are few (from 1 to 11 as identified for $a=0.556$, [19]) small oscillations around the connecting curve during one revolution in the bounding torus, that is, between two successive intersections with the Poincaré section.
[24] C. Letellier, Phys. Rev. Lett. **96**, 254102 (2006).
[25] O. E. Rössler, Phys. Lett. A **57**, 397 (1976).
[26] C. Letellier, G. Amaral, and L. A. Aguirre, Chaos **17**, 023104 (2007).
[27] L. A. Aguirre, E. C. Furtado, and L. A. B. Tôrres, Phys. Rev. E **74**, 066203 (2006).
[28] C. Letellier and L. A. Aguirre, Phys. Rev. E **79**, 066210 (2009).
[29] J. D. Farmer, J. P. Crutchfield, H. Fröling, N. H. Packard, and R. S. Shaw, Ann. N.Y. Acad. Sci. **357**, 453 (1980).
[30] O. E. Rössler, Bull. Math. Biol. **39**, 275 (1977).
[31] T. D. Tsankov and R. Gilmore, Phys. Rev. E **69**, 056206 (2004).
[32] T. D. Tsankov and R. Gilmore, Phys. Rev. Lett. **91**, 134104 (2003).
[33] A. M. Rucklidge, J. Fluid Mech. **237**, 209 (1992).
[34] C. Letellier, P. Dutertre, J. Reizner, and G. Gouesbet, J. Phys. A **29**, 5359 (1996).